Korean J Physiol Pharmacol 2019;23(5):317-328
https://doi.org/10.4196/kjpp.2019.23.5.317

KJPP

Original Article

Layer-specific cholinergic modulation of synaptic transmission in layer 2/3 pyramidal neurons of rat visual cortex

Kwang-Hyun Cho[1], Seul-Yi Lee[1], Kayoung Joo[1], and Duck-Joo Rhie[1,2,*]

[1]*Department of Physiology,* [2]*Catholic Neuroscience Institute, College of Medicine, The Catholic University of Korea, Seoul 06591, Korea*

ARTICLE INFO

Received February 13, 2019
Revised June 28, 2019
Accepted July 15, 2019

***Correspondence**
Duck-Joo Rhie
E-mail: djrhie@catholic.ac.kr

Key Words
Cholinergic modulation
Layer 2/3
Layer-specific
Synaptic transmission
Visual cortex

ABSTRACT It is known that top-down associative inputs terminate on distal apical dendrites in layer 1 while bottom-up sensory inputs terminate on perisomatic dendrites of layer 2/3 pyramidal neurons (L2/3 PyNs) in primary sensory cortex. Since studies on synaptic transmission in layer 1 are sparse, we investigated the basic properties and cholinergic modulation of synaptic transmission in layer 1 and compared them to those in perisomatic dendrites of L2/3 PyNs of rat primary visual cortex. Using extracellular stimulations of layer 1 and layer 4, we evoked excitatory postsynaptic current/potential in synapses in distal apical dendrites (L1-EPSC/L1-EPSP) and those in perisomatic dendrites (L4-EPSC/L4-EPSP), respectively. Kinetics of L1-EPSC was slower than that of L4-EPSC. L1-EPSC showed presynaptic depression while L4-EPSC was facilitating. In contrast, inhibitory postsynaptic currents showed similar paired-pulse ratio between layer 1 and layer 4 stimulations with depression only at 100 Hz. Cholinergic stimulation induced presynaptic depression by activating muscarinic receptors in excitatory and inhibitory synapses to similar extents in both inputs. However, nicotinic stimulation enhanced excitatory synaptic transmission by ~20% in L4-EPSC. Rectification index of AMPA receptors and AMPA/NMDA ratio were similar between synapses in distal apical and perisomatic dendrites. These results provide basic properties and cholinergic modulation of synaptic transmission between distal apical and perisomatic dendrites in L2/3 PyNs of the visual cortex, which might be important for controlling information processing balance depending on attentional state.

INTRODUCTION

Synaptic transmission and its neuromodulation are fundamental features of the nervous system. Synaptic transmission between excitatory pyramidal neurons constitutes a major cortical information flow while inhibitory transmission regulates transmission efficiency and integration properties of postsynaptic neurons [1]. In addition to a variety of cortical neurons, dendritic location of synapses in pyramidal neurons also adds a complexity of integration of synaptic transmission in the cortical network [2,3]. Theoretically, synapses located in distal dendrite exert less effect on somatic integration of all incoming synaptic activities than proximally located ones, although there are no general rules of local synaptic or global integration properties among cortical areas [4]. Modular construction of cortical columns and hierarchical connections between them, especially in the primary sensory cortex, has been suggested as a basic framework of cortical organization. Upstream and downstream connections between hierarchically organized cortical areas target discrete dendritic areas located in different cortical layers [5-7]. Thus, understanding the characteristics of synaptic transmission in different cortical layers would provide valuable information to understand cortical network.

Two major inputs to the primary sensory cortex come from the thalamus and upper brain areas, that convey sensory and

Author contributions: K.H.C., S.Y.L., and K.J. performed experiments and analysis. D.J.R. conceptualized and designed the study. K.H.C. and D.J.R. wrote the manuscript.

associative information, respectively. Sensory information from the thalamus is processed via layer 4, layer 2/3, and infragranular layers as the main excitatory intracortical connections. This input terminates mainly in perisomatic dendrites of layer 2/3 pyramidal neurons (L2/3 PyNs). Other major inputs from other brain areas including nearby cortex terminate on distal apical dendrites located in layer 1. This input constitutes about 25% of all synapses in L2/3 PyNs [8]. Thus, they are well suited for integrating these two kinds of information. It has been suggested that perisomatic input is the main driver of cortical pyramidal neurons while distal dendritic input modulates somatic integration of synaptic activities [9]. Since L2/3 PyNs receive sensory information from the thalamus directly and via layer 4 neurons in the primary visual cortex, they have been studied extensively as a model for the critical period of ocular dominance plasticity [10,11]. However, other inputs onto distal apical dendrites in layer 1 are less studied.

Neuromodulatory control of synaptic transmission is also layer specific [12,13]. It might differentially regulate sensory and associative synaptic transmission [14]. Cholinergic regulation of information flow between cortical areas during different brain states might be critical for many cognitive functions in the brain [15]. However, basic properties and neuromodulation of synaptic transmission in layer 1 is largely unknown. Previously, we have demonstrated that local stimulations of layer 1 and layer 4 mainly activate synapses in distal apical dendrites and perisomatic dendrites, respectively, in L2/3 PyNs of rat primary visual cortex [14]. Using this experimental configuration, we investigated basic properties of synaptic transmission in layer 1 of L2/3 PyNs in the present study. Additionally, layer-specific cholinergic modulation on different synaptic inputs was studied. Our findings provide basic properties of synaptic transmission in layer 1. Results of this study suggest that layer-specific differential cholinergic modulation may regulate information transfer balance between sensory and associative pathways depending on brain states.

METHODS

Slice preparation

Coronal slices of primary visual cortex were prepared from Sprague-Dawley rats (Orientbio Inc., Seongnam, Korea) on their postnatal days 21 to 27. Animal cares and surgical procedures were performed after receiving approval of the Institutional Animal Care and Use Committee (IACUC) in the Catholic University of Korea (IACUC approval No. 2019-0024-01). Animals were sedated with chloral hydrate (400 mg/kg, i.p.). After decapitation, brains were quickly removed and then immersed in ice-cold artificial cerebrospinal fluid (ACSF) containing (in mM) 125 NaCl, 2.5 KCl, 25 $NaHCO_3$, 1.25 NaH_2PO_4, 1 $CaCl_2$, 2 $MgSO_4$, and 10 D-glucose and aerated with a mixture of 95% O_2 and 5% CO_2. Coronal sections (300-μm thick) were prepared with a vibroslicer (HM650V; Microm, Walldorf, Germany) and allowed to recover in a submerged slice chamber for 30 min at 37°C. These slices were then maintained at room temperature (22°C–24°C) in the same ACSF before use. Slices were individually transferred to the recording chamber and superfused continuously (1–1.5 ml/min) with the same aerated solution, except for the addition of 2 mM $CaCl_2$ and 1 mM $MgSO_4$. The temperature of the bath solution in the recording chamber was maintained at 31°C–32°C.

Whole-cell patch-clamp recording

Whole-cell patch-clamp recording was performed as described previously [12]. L2/3 PyNs of the primary visual cortex were identified under infrared-DIC video-microscopy with an upright microscope (BX51-WI fitted with a 40×/0.80 NA water immersion objective; Olympus, Tokyo, Japan). Whole-cell recording was obtained with a Multiclamp 700B amplifier (Molecular Devices, Union City, CA, USA) and a pClamp 10.3 software (Axon Instruments, Inc., Forster City, CA, USA). Data were low-pass filtered at 5 kHz and sampled at 20 kHz. Patch electrodes (3–5 MΩ) were filled with K-gluconate based intracellular solution containing (in mM) 130 K-gluconate, 10 KCl, 4 Mg-ATP, 10 Na_2-phosphocreatine, 0.3 Na_3-GTP, and 10 *N*-2-hydroxyethylpiperazine-*N*′-2-ethanesulfonic acid (HEPES) (pH 7.25 with KOH) to record excitatory postsynaptic current (EPSC), excitatory postsynaptic potential (EPSP), and miniature EPSC (mEPSC). Typical access resistance was 12–15 MΩ determined by the Axoclamp bridge balance circuitry. To record inhibitory postsynaptic current (IPSC) and miniature IPSC (mIPSC), pipettes were filled with a CsCl-based solution containing (in mM) 145 CsCl, 4 Mg-ATP, 10 Na_2-phosphocreatine, 0.3 Na_3-GTP, and 10 HEPES (pH 7.25 with CsOH). Calculated junction potentials for K-gluconate- and CsCl-based pipette solutions were 14 and 4 mV, respectively. They were not corrected. EPSC(P) and IPSC were evoked by applying extracellular stimulation (0.1-ms duration) with bipolar tungsten electrodes (100 μm in diameter, SNE-100; David Kopf, Tujunga, CA, USA) or a glass pipette (20-μm tip diameter) filled with ACSF using a constant-current isolation unit (A360; World Precision Instruments, Sarasota, FL, USA). Stimulation intensities were adjusted to evoke 90–200 pA of postsynaptic currents. Electrodes for stimulation of layer 1 were positioned ~150 μm laterally to the soma. Layer 4 electrodes were positioned 500–600 μm from the pial surface. Both mEPSC and mIPSC were recorded in the presence of tetrodotoxin (1 μM). To record IPSC and mIPSC, 6,7-dinitroquinoxaline-2,3-dione disodium salt (DNQX) (20 μM) and D-(-)-2-Amino-5-phosphonopentanoic acid (D-AP5) (50 μM) were added to ACSF. Paired-pulse ratio (PPR) was determined as the amplitude of the second EPSC to that of the first EPSC evoked by paired-pulse stimulation (10- to 200-ms interval). Amplitudes of second EPSCs were measured from single exponential fit of first EPSCs. In some experiments, glutamate (0.3–3 mM) was puff-applied with a Picospritzer III (Parker Instrumentation,

Cleveland, OH, USA) every 20 sec via a glass pipette (5-μm diameter, 5 psi, 5–30 ms) to monitor postsynaptic response. The puff pipette was located either near the soma (~50 μm from the soma) or in layer 1 (~100-μm lateral to the soma). Miniature events were detected based on a template response from spontaneous signal and searched automatically using Clampfit software (Axon Instruments, Inc.) or Mini analysis software (Synaptosoft, Inc., Decatur, GA, USA). Automatically selected events were visually monitored to discard erroneous noises. Both frequency and the amplitudes of events were analyzed.

Ratio for AMPA/NMDA receptor-mediated EPSCs and rectification index

Neurons were recorded at −80 mV to isolate AMPA receptor-mediated EPSC, and at +40 mV to isolate NMDA receptor-mediated EPSC [16]. After obtaining stable EPSCs, 50 μM D-AP5 was applied to ACSF for 8 min. EPSCs were obtained again and then 20 μM DNQX was applied additively to ACSF for 8 min. All ACSFs contained 10 μM bicuculline to isolate EPSCs from inhibitory component. AMPA receptor- and NMDA receptor-mediated EPSCs were then isolated and analyzed following off-line subtraction. The amplitude of AMPA receptor-mediated EPSC was taken at the peak of synaptic response recorded at −80 mV. The amplitude of NMDA receptor-mediated EPSC was taken 50 ms after stimulus onset at +40 mV when AMPA-EPSC component decayed to baseline. The ratio of AMPA/NMDA receptor-mediated EPSC was then obtained from these values.

Rectification index of AMPA receptor-mediated EPSCs was obtained at the stage for application of D-AP5 in bicuculline containing ACSF. Current–voltage (I–V) relationship of AMPA receptor-mediated EPSCs was measured at various membrane potentials (−80, −40, −20, 0, 20, 40 mV) and then plotted using peak amplitude of EPSCs measured at each membrane potential. Reversal potential for AMPA receptor mediated-EPSC (E_{rev}) was obtained using linear fitting curve from its I–V relationship. Liquid junction potential was offline-corrected. Rectification index (RI) was calculated using the following equation: RI = I_{+40} / (40 − E_{rev}) / I_{-40} (E_{rev} + 40). In these experiments for ratio of AMPA/NMDA receptor-mediated EPSCs and rectification index, all currents were measured using Cs-gluconate-based pipette solution containing (in mM) 135 Cs-gluconate, 10 CsCl, 4 Mg-ATP, 0.3 Na_3-GTP, 10 Na_2-phosphocreatine, 10 HEPES, and 3 QX-314 (pH 7.27 by CsOH) with 50 unit/ml creatine phosphokinase.

Drugs

D-AP5, DNQX, tetrodotoxin, and N,2,3,3-tetramethylbicyclo[2.2.1]heptan-2-amine hydrochloride (Mecamylamine) were purchased from Tocris Bioscience (Bristol, UK). All other chemicals were purchased from Sigma-Aldrich (St Louis, MO, USA).

Statistical analysis

Data are expressed as mean ± standard error (SE). Statistical comparisons were performed with paired or unpaired two-tailed Student's t-test and analysis of variance (ANOVA) using Excel and/or SigmaStat (Systat software Inc., Chicago, IL, USA). The level of significance was set at $p < 0.05$.

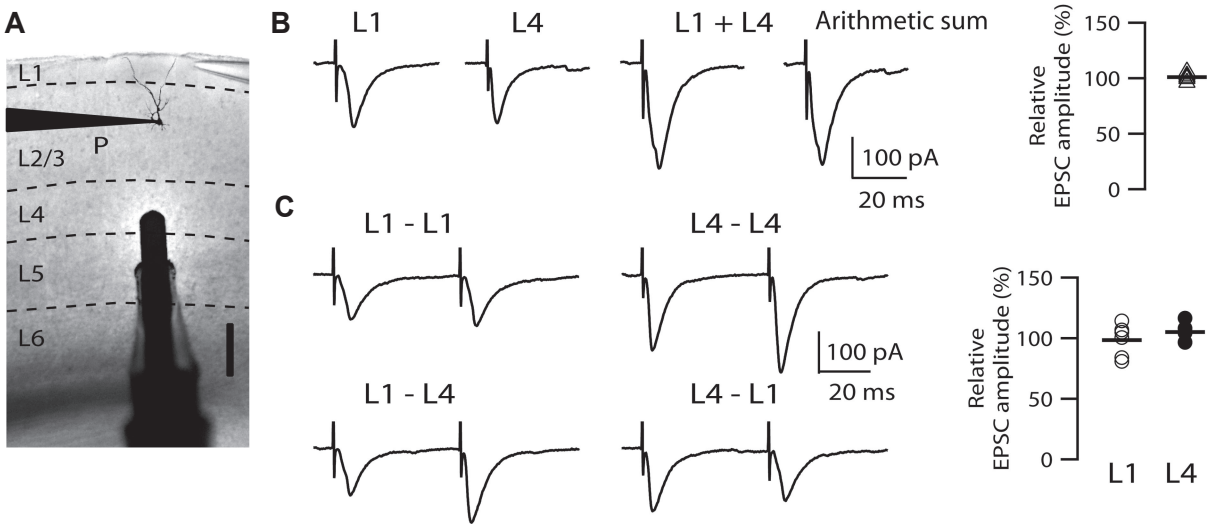

Fig. 1. Independency of layer 1 (L1) and L4 stimulations. (A) Experimental configuration (5x objective image) showing positions of glass and tungsten electrodes at L1 and L4, respectively. A patch pipet recording a layer 2/3 pyramidal neuron was indicated as P. Image of biocytin-filled cell is overlaid. Scale = 200 μm. (B) Excitatory postsynaptic currents (EPSCs) evoked by combined stimulation of L1 and L4 (L1 + L4) were compared with the arithmetic sum of each EPSC (*right panel*, n = 5). (C) Cross paired-pulse stimulation of L1 and L4 stimulations indicated the independency of these two inputs. Relative EPSC amplitude was obtained from peak amplitude of the second EPSC of cross paired-pulse stimulation (L1–L4, L4–L1) versus peak amplitude of the first EPSC of paired-pulse stimulation (L1–L1, L4–L4) (n = 6).

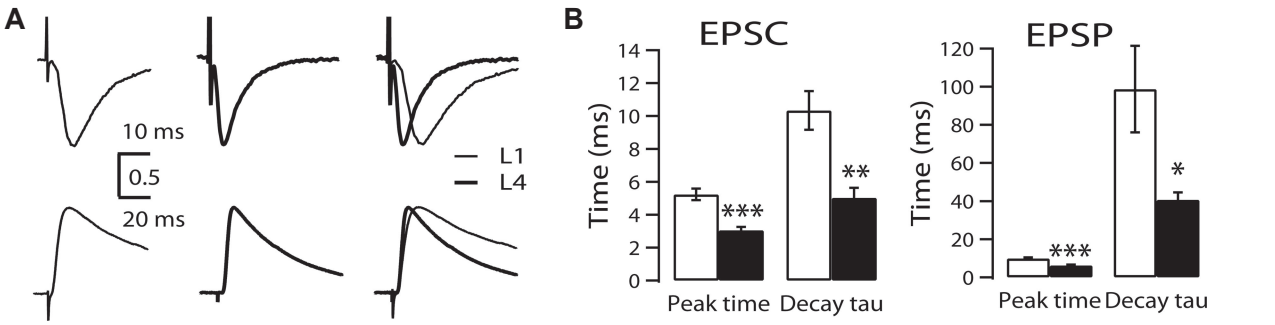

Fig. 2. Kinetics of excitatory postsynaptic current (EPSC) and excitatory postsynaptic potential (EPSP) evoked by layer 1 (L1) and L4 stimulations. (A) EPSCs (*upper traces*) and EPSPs (*lower traces*) were recorded with stimulations of L1 (thin trace) and L4 (thick trace). EPSC(P) traces were normalized to the peak. (B) Summary plots of peak time and decay time constant (tau) of EPSC (n = 11) and EPSP (n = 9) evoked by stimulations of L1 (open bar) and L4 (closed bar). *p < 0.05, **p < 0.01, ***p < 0.001 compared to L1.

RESULTS

Stimulations of layer 1 and layer 4 activated independent sets of synapses

Whole-cell patch-clamp recordings were performed under either voltage- or current-clamp mode in L2/3 PyNs of the primary visual cortex from 3-week-old rats. EPSC was evoked by extracellular stimulation of layer 1 ~150 μm lateral from the soma or underlying layer 4 as shown in Fig. 1A. We have previously reported that these two local stimulations-activated synapses are located mainly in distal apical dendrite in layer 1 and perisomatic area in layer 2/3, respectively [14]. In Fig. 1 we demonstrated two stimulations activated independent inputs. The peak amplitude of EPSC evoked by simultaneous stimulation of layers 1 and 4 was similar to the arithmetic sum of those evoked by each stimulation (101.0 ± 1.6%, n = 5, p = 0.587) (Fig. 1B). The amplitude of the second EPSCs of cross-paired stimulation (L1–L4 and L4–L1) was unchanged from that of the first EPSCs of paired stimulation (L1–L1 and L4–L4) (L1: 98.5 ± 5.4%, n = 6, p = 0.798; L4: 105.0 ± 3.1%, n = 6, p = 0.169) (Fig. 1C).

We then compared kinetics of EPSCs and the resulting EPSPs evoked by stimulation of layers 1 and 4 recorded in the same neurons. Peak time and decay tau of EPSCs evoked by stimulation of layer 1 (L1-EPSCs) were 5.24 ± 0.35 ms (n = 11) and 10.34 ± 1.17 ms, respectively. Peak time and decay tau of L4-EPSCs were 3.06 ± 0.20 ms (p < 0.001 compared with L1-EPSC) and 5.04 ± 0.61 ms (p < 0.01 compared with L1-EPSC), respectively (Fig. 2). Peak time and decay tau of L1-EPSP were 9.89 ± 0.47 ms (n = 9) and 98.80 ± 22.75 ms, respectively. L4-EPSP showed faster kinetics both in peak time (6.29 ± 0.46 ms, p < 0.001) and decay tau (40.68 ± 3.84 ms, p < 0.05) than L1-EPSP. This suggested that L1-EPSP was spatially filtered by long apical dendrites of L2/3 PyNs. These results, in addition to our previous imaging data with unloading of FM1-43 dye [14], indicated that these two local stimulations activated synapses of two independent sets, located in distal apical and perisomatic dendrites, respectively.

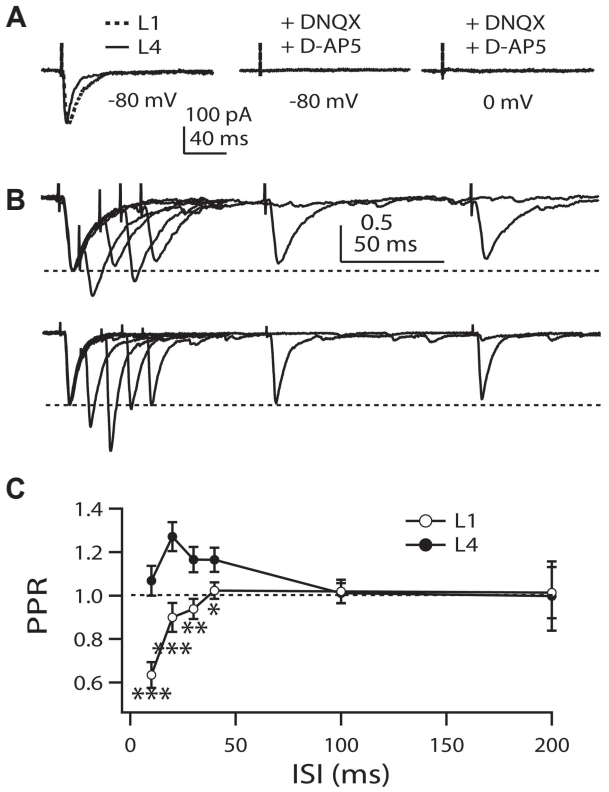

Fig. 3. Short-term kinetics of excitatory postsynaptic current (EPSC) evoked by layer 1 (L1) and L4 stimulations. (A) Left panel shows representative currents evoked by stimulations of L1 (dotted line) and L4 (solid line) recorded at holding potential of –80 mV. Middle and right panels show representative currents measured at holding potential of –80 mV and 0 mV, respectively, in the presence of 6,7-dinitroquinoxaline-2,3-dione disodium salt (DNQX) (20 μM) and D-(-)-2-Amino-5-phosphonopentanoic acid (D-AP5) (50 μM) in bath solution (n = 3). (B) Representative traces from paired-pulse stimulations with interstimulus interval (ISI) of 10 to 200 ms, evoked by L1 stimulation (*upper traces*) and L4 stimulation (*lower traces*). EPSC traces were normalized to the first peak. (C) Summary of paired-pulse ratio (PPR) with stimulations of L1 and L4 (n = 13). *p < 0.05, **p < 0.01, ***p < 0.001 compared to L4.

Differential paired-pulse ratio between layer 1 and layer 4 inputs

To investigate presynaptic properties terminating on distal apical and perisomatic inputs, we recorded PPR with various interstimulus intervals (ISI) (Fig. 3). Complete inhibition of EPSCs in the presence of DNQX and D-AP5 indicated that EPSC was mediated by AMPAR- and NMDAR-type glutamate receptors (Fig. 3A). Stimulus intensity was set to evoke ~90 pA in both inputs (n = 13, p = 0.621). PPRs of layer 1 stimulation with ISI of 10 ms (100 Hz) were depressing, while those of layer 4 stimulation with ISI from 20 ms (50 Hz) to 40 ms (25 Hz) were facilitating (Fig. 3B). Thus, L4-EPSC was more facilitating than L1-EPSC at ISI ≤ 40 ms (Fig. 3C). These results indicate that presynaptic release probability differs between synapses terminating on distal apical and perisomatic dendrites, implying that high frequency firing of sensory inputs (≥ 25 Hz) is more facilitating to evoke action potentials than that of associative inputs.

Differential cholinergic modulation of synaptic transmission between distal apical and perisomatic dendrites

Acetylcholine (ACh) level in the cortex released by cholinergic fibers originating from the basal forebrain varies depending on brain state such as attention and sleep cycle [17]. It has been proposed that ACh level may control information flow between sensory and associative pathways as ACh is involved in learning during attention and memory consolidation during deep sleep [17]. Thus, we studied nicotinic and muscarinic modulation of synaptic transmission between distal apical and perisomatic dendrites (Fig. 4). Bath application of muscarine decreased L1-EPSCs (n = 8, p < 0.001) and L4-EPSCs (n = 8, p < 0.001) in a concentration-dependent manner. EC_{50} in L4-EPSC (0.86 μM) was lower than that in L1-EPSC (2.26 μM). On the other hand, application of nicotine failed to change the amplitude of L1-EPSC (n = 8). However, it increased L4-EPSC by ~20% at the concentration of 0.1 μM (p < 0.05), which was maintained up to 10 μM (n = 9). Non-specific cholinergic agonist carbachol showed inhibitory effect similar to that of muscarine between two inputs (L1: n = 12, EC_{50} = 4.91 μM; L4: n = 14, EC_{50} = 4.19 μM). These results indicate that muscarinic activation can potently decrease synaptic transmission in both pathways with lower EC_{50} in sensory pathway while nicotinic activation can efficiently increase synaptic transmission specifically in sensory pathway. Thus, cholinergic stimulation may differentially modulate sensory and associative pathways. Measurement of PPR could provide an indirect evidence of pre- or post-synaptic mechanism of neuromodulators. Thus, PPR was measured in the presence or absence of muscarine. PPR (50-ms interval) was changed by bath application of muscarine from 0.89

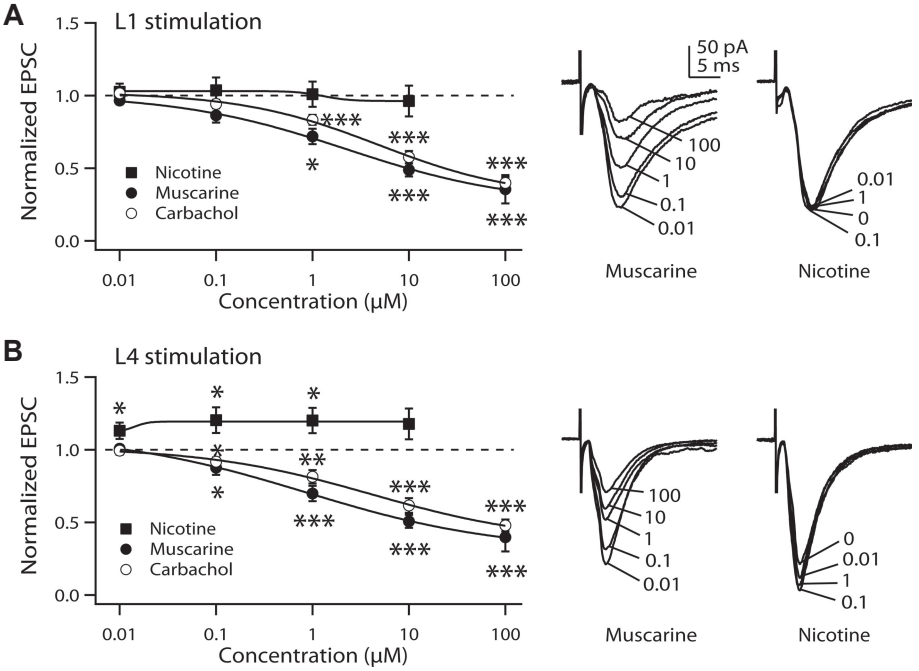

Fig. 4. Cholinergic modulation of excitatory postsynaptic current (EPSC) evoked by layer 1 (L1) and L4 stimulations. EPSCs were evoked by stimulations of L1 (A) and L4 (B) with bath application of cholinergic agonists at various concentrations. Representative traces of EPSC at various concentrations (μM) of muscarine and nicotine are shown in the right panel. All drugs were applied into bath solution and effects were analyzed at 5 min after application of the drugs (n = 8–14). EPSCs were decreased by non-specific cholinergic agonist carbachol and muscarinic receptor agonist muscarine in a concentration-dependent manner. However, nicotinic receptor agonist nicotine increased L4-EPSC at concentrations lower than 1 μM. *p < 0.05, **p < 0.01, ***p < 0.001 compared with normal bath solution.

± 0.04 to 1.05 ± 0.04 in L1 (n = 8, p < 0.01) and 1.01 ± 0.04 to 1.19 ± 0.07 in L4 (n = 8, p < 0.05), respectively. This result supports presynaptic nature of muscarinic modulation.

Although visual cortical slices were disconnected from the basal forebrain, cholinergic axons in these slices might modulate baseline transmission in control condition. We examined these possibilities with bath application of atropine (10 μM) and the non-specific nicotinic antagonist mecamylamine (30 μM) for 10 min. These procedures did not change baseline synaptic transmission evoked by stimulation of L1-EPSC or L4-EPSC (data not shown). Muscarinic inhibition of synaptic transmission appears to be presynaptic via M2/M4 receptor subtypes. We confirmed this with puff-application of glutamate (Fig. 5). A glass pipette (5 μm in diameter) for puff application of glutamate was positioned in layer 1 and near the soma to stimulate synapses in distal apical and perisomatic dendrites, respectively (Fig. 5A). Amplitude of EPSC evoked by puff-applied glutamate was set to be similar to that by extracellular stimulation as shown in Fig. 1 (~90 pA). Bath application of the cholinergic agonist carbachol (10 μM), muscarine (10 μM), and nicotine (10 μM) failed to affect the amplitude of EPSC evoked by puff application of glutamate (0.3–3 mM) in layer 1 or perisomatic area (n = 5). Provided that puff application substantially caused dilution in local milieu of brain slice and that it affected glutamate-induced EPSC, decay kinetics for glutamate-evoked EPSC might have been changed. However, there was no difference in decay time constant for glutamate-evoked EPSC between control and ACh derivatives by puff application (L2/3: 62.2 ± 6.9 ms in control, 74.1 ± 7.8 in muscarine, p = 0.218, n = 7; L1: 73.1 ± 25.3 ms in control, 69.5 ± 21.7 ms in muscarine, p = 0.390, n = 5). Thus, possible dilution effect of puff application could be excluded. We then examined the inhibitory effect of muscarine on mEPSC in the presence of tetrodotoxin (1 μM). As shown in Fig. 5D and E, the amplitude of mEPSC (11.1 ± 0.8 pA to 10.7 ± 0.8 pA, n = 10, p = 0.246) was not changed by the application of muscarine (10 μM) while the frequency of mEPSC was decreased by 36% (5.0 ± 0.6 Hz to 3.2 ± 0.4 Hz, n = 11, p < 0.001). Thus, muscarinic and nicotinic modulation of synaptic transmission as shown in Fig. 4 was caused by exclusively presynaptic effect.

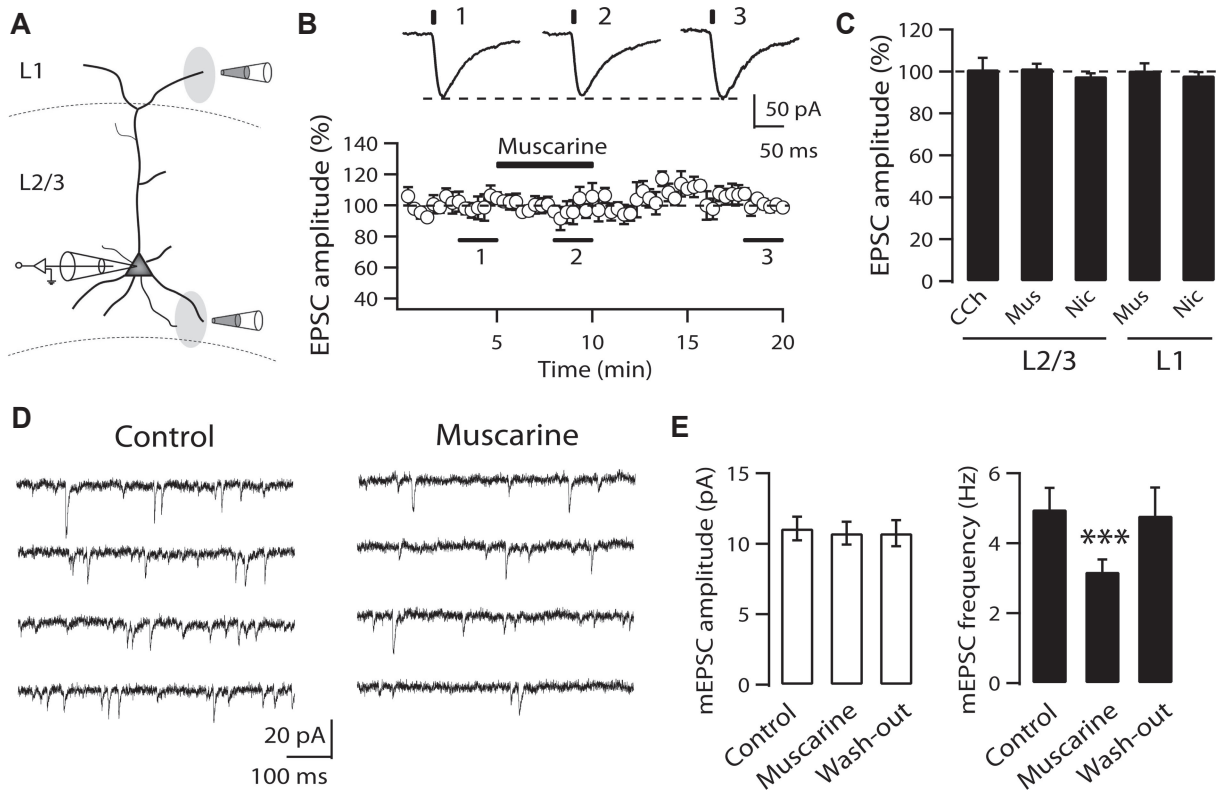

Fig. 5. Presynaptic effect of cholinergic modulation on excitatory postsynaptic current (EPSC). (A) Experimental configuration showing positions of glass puff-pipettes (layer 1 [L1] and L2/3) and a recording patch pipet with an L2/3 pyramidal neuron. (B) Inward currents were evoked by puff application of glutamate (0.3–3 mM) in L1 and L2/3 (perisomatic area). Puffs were applied every 20 sec at 5 psi for 5–30 ms using a glass pipet (bars on traces). Muscarine (10 μM, 5 min) was applied into the bath solution. Upper traces show representative average EPSCs taken at indicated time period (2 min). (C) Summary plot for effects of various cholinergic agonists (10 μM) on amplitude of EPSCs evoked by puff application of glutamate (n = 5) recorded at the end of application (CCh, carbachol; Mus, muscarine; Nic, nicotine). (D) Representative traces of muscarine (10 μM) application on miniature EPSCs (mEPSCs) recorded in the presence of tetrodotoxin (1 μM). (E) Summary plots of muscarine effects on mEPSCs amplitude and frequency (n = 11). ***p < 0.001 tested with ANOVA.

Layer-specific cholinergic modulation of inhibitory transmission in L2/3 PyNs

Local inhibitory interneurons control synaptic integration and excitability of cortical neurons. Axons from specific types of inhibitory interneurons innervate subcellular region of pyramidal neurons depending on cortical layers [18]. Thus, we also investigated layer-specific characteristics and neuromodulation of inhibitory transmission in L2/3 PyNs. In contrast to PPR of EPSCs, PPR was similar in IPSCs evoked by layer 1 and layer 4 stimulations (Fig. 6). Although PPR was depressed at ISI of 10 ms, paired pulse failed to change the second IPSCs in both inputs at ISI of > 20 ms. Application of nicotine failed to change the amplitude of IPSCs evoked by layer 1 and layer 4 stimulations (Fig. 7). Application of muscarine inhibited IPSCs in a concentration-dependent manner ($p < 0.001$). This effect was similar between layer 1 and perisomatic synapses. Application of carbachol also inhibited IPSCs evoked layer 1 and layer 4 stimulations in a concentration-dependent manner. Frequency (5.2 ± 0.7 Hz to 4.1 ± 0.6 Hz, n = 8, $p < 0.001$) but not amplitude (25.6 ± 2.2 pA to 25.1 ± 2.7 pA, $p = 0.817$) of mIPSC was changed by the application of muscarine (10 μM), implying presynaptic inhibition of probability of vesicle release. Thus, in contrast to EPSCs, there was no layer-specific cholinergic modulation in inhibitory synaptic transmission of L2/3 PyNs.

AMPA/NMDA currents in distal apical and perisomatic synapses

Composition of AMPA and NMDA receptor subtypes and AMPA/NMDA ratio can change with postnatal maturation in

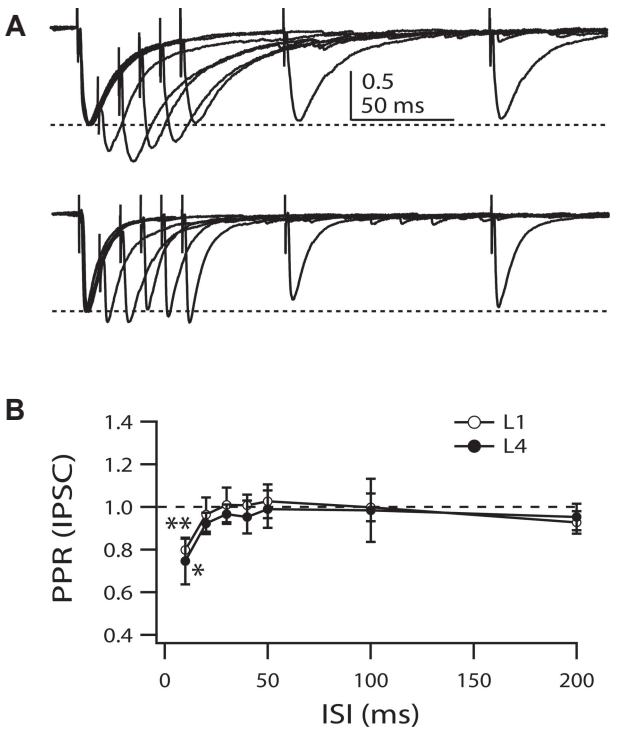

Fig. 6. Short-term kinetics of inhibitory postsynaptic current (IPSC) evoked by layer 1 (L1) and L4 stimulations. IPSCs were evoked by paired-pulse stimulation with various interstimulus interval (ISI) with L1 and L4 stimulations in the presence of 6,7-dinitroquinoxaline-2,3-dione disodium salt (DNQX) (20 μM) and D-(-)-2-Amino-5-phosphonopentanoic acid (D-AP5) (50 μM). (A) Representative IPSCs evoked by paired-pulse stimulations with ISI of 10 to 200 ms, evoked by L1 stimulation (*upper traces*) and L4 stimulation (*lower traces*). IPSC traces were normalized to the first peak. (B) Summary plot shows paired-pulse ratio (PPR) with L1 stimulation (n = 14) and L4 stimulation (n = 16). *$p < 0.05$, **$p < 0.01$ tested with ANOVA.

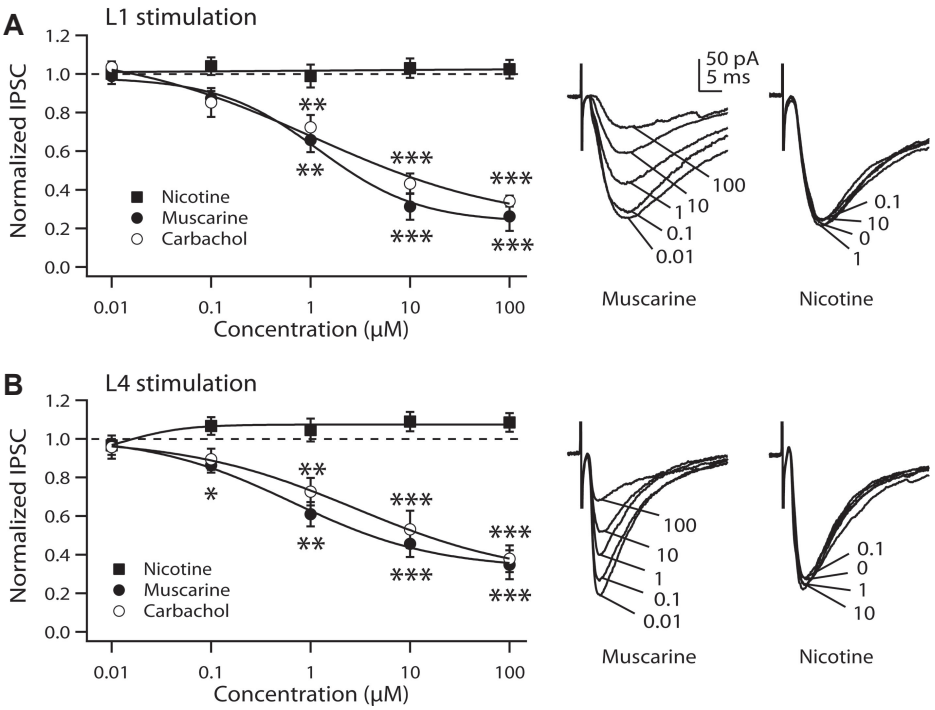

Fig. 7. Cholinergic modulation of inhibitory postsynaptic currents (IPSCs) evoked by layer 1 (L1) and L4 stimulations. IPSCs were evoked by stimulating L1 (A) and L4 (B) in the presence of various cholinergic agonists. Representative traces of inhibitory postsynaptic current (IPSC) at various concentrations (μM) of muscarine and nicotine were shown in the right panel. All drugs were applied in the bath solution and their effects were analyzed at 5 min after application. IPSCs were declined by carbachol (n = 10) and muscarine (n = 7) in a concentration-dependent manner. Nicotine had no effects on L1 or L4 stimulation (n = 8). *$p < 0.05$, **$p < 0.01$, ***$p < 0.001$ compared with normal bath solution.

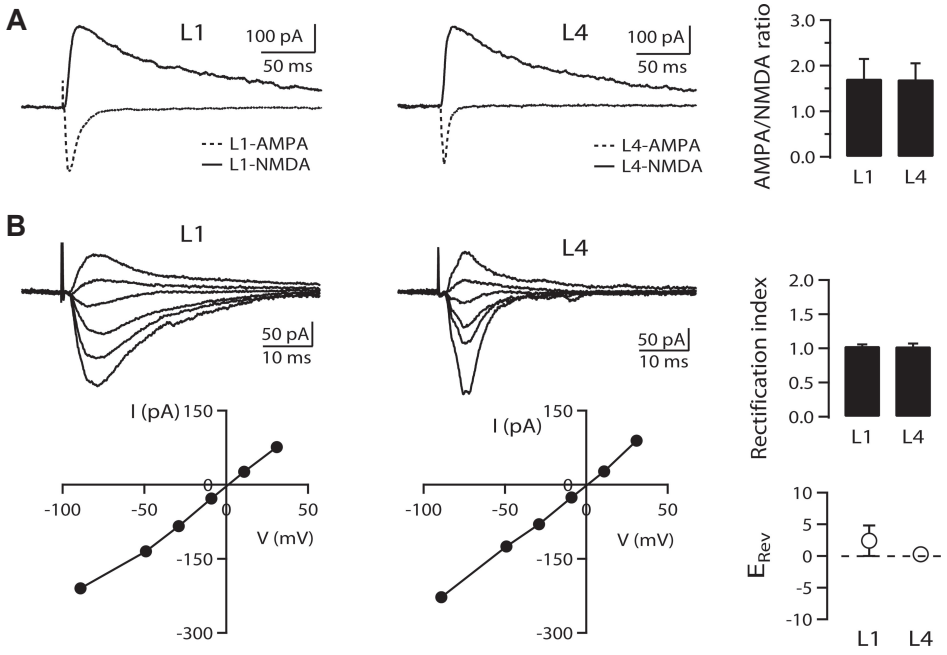

Fig. 8. Properties of glutamatergic synapses activated by layer 1 (L1) and L4 stimulations. (A) Excitatory postsynaptic currents (EPSCs) were evoked by L1 stimulation (*left panel*) or L4 stimulation (*middle panel*) at holding potential of either –80 or +40 mV. Amplitude of AMPA receptor-mediated EPSC was analyzed at peak of synaptic response recorded at –80 mV (dotted line). Amplitude of NMDA receptor-mediated EPSC was analyzed 50 ms after stimulus onset at +40 mV (solid line). Ratio of AMPA/NMDA receptor-mediated EPSCs was obtained from these values (*right panel*, n = 5–7). (B) AMPA receptor-mediated EPSCs were measured at various membrane potentials. Current–voltage (I–V) curve of L1 (*left panels*) and L4 stimulation (*right panels*) are plotted. Rectification index of AMPA receptor-mediated EPSCs was calculated using the following equation: I_{+40} / (40 – E_{rev}) / I_{-40} (E_{rev} + 40). Reversal potential for AMPA receptor mediated-EPSC (E_{rev}) was obtained from its I–V relationship.

the primary sensory cortex [19,20] which is responsible for critical period of the primary visual cortex [21]. Since ocular dominance and synaptic plasticity are also layer specific, we investigated differences in properties of glutamatergic transmission between layer 1 and perisomatic synapses. GluR2-lacking AMPA receptors expressed during early postnatal ages are calcium permeable. Inward rectification is a characteristic feature of those receptors. There was no rectification in distal apical (rectification index = 1.04 ± 0.02, n = 5) or perisomatic synapses (rectification index = 1.03 ± 0.04, n = 7, p = 0.895) in L2/3 PyNs from 3-week-old rats (Fig. 8). Reversal potential was similar between distal apical (2.4 ± 1.6 mV) and perisomatic (0.3 ± 0.5 mV) synapses (p = 0.207). Membrane expression of AMPA receptors in NMDA receptors-abundant silent synapses is also important for postnatal maturation of glutamatergic synapses. As shown in Fig. 8A and B, AMPA/NMDA ratios did not differ between distal apical (1.72 ± 0.43, n = 5) and perisomatic (1.70 ± 0.35, n = 7) synapses in 3-week-old rats (p = 0.979). These results indicate that molecular compositions of AMPA and NMDA receptors are similar between distal apical and perisomatic dendrites in L2/3 PyNs of the primary visual cortex.

DISCUSSION

We investigated differential properties and cholinergic modulation of excitatory and inhibitory synaptic transmission between distal apical and perisomatic dendrites in L2/3 PyNs of the rat visual cortex. EPSC evoked by local electrical stimulation of layer 1 activating distal apical synapses showed slower kinetics than that by layer 4 stimulation activating perisomatic dendrites. Excitatory synapses in distal apical dendrites showed presynaptic depression while those in perisomatic dendrites were facilitating. In contrast, IPSCs showed similar PPR between layer 1 and layer 4 stimulations with depression only at 100 Hz. Cholinergic stimulation induced presynaptic depression by activating muscarinic receptors in excitatory and inhibitory synapses to similar extents in both inputs. However, nicotinic stimulation enhanced excitatory synaptic transmission by ~20% only in inputs activated by layer 4 stimulation. Molecular compositions of AMPA receptors and AMPA/NMDA ratio were similar between synapses in distal apical and perisomatic dendrites. These results provide basic properties and cholinergic modulation of synaptic transmission between distal apical and perisomatic dendrites in L2/3 PyNs of the visual cortex.

Basic synaptic properties located in different dendritic compartments

Cortical pyramidal neurons are major excitatory neurons located in all six cortical layers except layer 1. Among them, L2/3 and layer 5 (L5) are characterized by long apical dendrites extending to layer 1, where they branch richly and form the so called apical tuft [22]. Perisomatic dendrites including basal dendrites constitute another dendritic domain [4]. Due to the long distance from the soma up to 1 mm in rat cortex in the case of L5 PyNs, apical dendritic synapses appear to act as modulating inputs in contrast to perisomatic inputs [9]. In the present study, we applied local electrical stimulations at layers 1 and 4 to activate synapses located in distal apical and perisomatic dendrites, respectively, which was confirmed in our previous study [14]. In the present study, we further confirmed that these two stimulations activated independent inputs (Fig. 1) and that L1-EPSC and L1-EPSP showed slower kinetics than L4-EPSC and L4-EPSP (Fig. 2). This indicated that L1-EPSC was electrotonically more filtered than L4-EPSC due to long apical dendrites. Paired-pulse stimulation with various interstimulus intervals in L1 showed short-term depression while that in L4 exhibited short-term facilitation (Fig. 3). Generally, short-term facilitation is a characteristic feature of low-probability synapses while short-term depression is a property of synapse with high release probability [23]. Thalamocortical synapses having high release probability tend to show short-term depression in layer 4 neurons in mouse somatosensory cortex [24]. Although layer 4 stimulation appears to activate thalamocortical synapse in the present study, the discrepancy might be due to different areas and pyramidal neurons in different layers. Different temporal summation profiles in response to repetitive presynaptic activities between distal apical and perisomatic dendrites suggest different release probability, which may affect dendritic integration property between associative and sensory information [25-28].

Different sets of inhibitory interneurons are innervated in different dendritic compartment of cortical pyramidal neurons [18]. In contrast to excitatory synaptic transmission, however, IPSC evoked by layer 1 and layer 4 stimulations showed paired-pulse depression to a similar extent (Fig. 6). Although inclusion of inhibitory synaptic transmission in our stimulations was minimal (Fig. 3A), if any, these results also corroborated our results (Fig. 4) showing that the difference in paired-pulse response of EPSC between layer 1 and 4 stimulation was not resulted from changes in inhibitory transmission.

Differential cholinergic modulation of synaptic transmission between distal apical and perisomatic dendrites

Synaptic transmission in the brain is regulated by neuromodulators that vary with brain state [29]. It has been hypothesized that different acetylcholine levels control balance between sensory and associative information flow [15]. In the hippocampus and neocortex, high acetylcholine level during attention enhances input to encode while low acetylcholine level during deep sleep enhances feedback to consolidate [30]. The entire cerebral cortex including the hippocampus is diffusely innervated by cholinergic fibers from the basal forebrain [31,32]. Muscarinic and nicotinic receptors are distributed in all cortical layers [28,33,34]. In the present study, cholinergic agonist carbachol and muscarine similarly decreased excitatory synaptic transmission in distal apical and perisomatic dendritic compartments. Muscarinic suppression of EPSC and IPSC was likely to be presynaptic (Fig. 5), in agreement with previous finding showing that presynaptically located M2/M4 subtypes suppressed neurotransmitter release probability [33]. We analyzed rise time of mEPSC in both control and muscarine condition to identify the layer specific nature of mEPSC. Rise time of mEPSC was distributed from 0.2 ms to 1.5 ms, which was not changed after application of muscarine. However, rise time of mEPSC could not be a parameter for layer-specific localization of synapses because distal basal dendrites are long enough as apical dendrites. Thus, we could not pursue the origin of mEPSC or their layer-specific modulations with rise time of mEPSC. Meanwhile, nicotinic activation increased EPSC amplitude by ~20% only in perisomatic dendritic area. In a previous study, similar muscarinic and nicotinic modulations of transmission between intracortical and thalamocortical synapses in the barrel cortex were found [24]. Both intracortical and thalamocortical excitatory synapses were depressed by activation of muscarinic receptors. Nicotine was slightly enhanced thalamocortical input. In olfactory cortex, intrinsic synaptic response was strongly reduced by muscarinic activation whereas afferent input was not affected [35]. Although muscarine inhibited both thalamocortical and intracortical inputs, intracortical input was more susceptible than thalamocortical input in auditory cortex [36]. *In vivo* experiment, muscarine depressed both intracortical and sensory input while nicotine enhanced only sensory input by stimulating whiskers in barrel cortex [37]. Although nicotinic activation enhanced excitatory transmission only in perisomatic inputs even at a low concentration (0.1 μM), synaptic transmissions were potently suppressed by carbachol. Since acetylcholine acts on both nicotinic and muscarinic receptors simultaneously, acetylcholine may not enhance synaptic transmission in perisomatic sensory inputs via nicotinic activation only *in vivo*. Beside this short-term regulation of synaptic transmission, long-term synaptic plasticity is also critical in setting information flow balance between sensory and associative pathways in the cortex. In our previous study, cholinergic stimulation induced long-term potentiation (LTP) or long-term depression (LTD) depending on Ca^{2+} release from stores in basal dendrites, but only LTD was induced in distal apical dendrites without Ca^{2+} release [12]. In addition, serotonin related to mood evoked short-term facilitation in inhibitory transmission only in layer 1 inputs [38]. Thus, studies on cellular and molecular mechanisms involving layer-

specific modulation of synaptic transmission are warranted in the future. Excitation and inhibition balance (E-I balance) in synaptic transmission might be important for information flow in cortical circuit [39,40]. Endogenously released ACh amplifies the dominance of inhibitory drive but decreases excitability and sensory responsiveness of layer 5 pyramidal neurons [41]. Studies about cholinergic effects on E-I balance are also warranted in the future.

Molecular composition of glutamate synapses in layer 1

Stratum radiatum interneurons in the hippocampus express GluR2-deficient AMPA receptors that are Ca^{2+}-permeable. They can also induce long term synaptic plasticity [42]. In the neocortex, GluR2-lacking AMPA receptors can switch to GluR2-containing AMPA receptors during early postnatal development [43]. This maturation of AMPA receptors is also layer dependent around postnatal day 13 to 15 in the primary somatosensory cortex of rats [19]. Expression of AMPA receptors into NMDA receptor-only silent synapses is also developmentally regulated, coinciding with switch of GluR2-lacking AMPA receptors: NMDA/AMPA ratio in basal dendrites of L2/3 PyNs from rat somatosensory cortex decreases around postnatal day 12 [44]. These developmental changes have been studied in major cortical circuits involving sensory processing (thalamus → layer 4 → layer 2/3 → layer 5). However, properties of synaptic transmission in cortical layer 1 sending associative inputs remain unclear. In the present study, we investigated rectification index for GluR2-lacking synapses and NMDA/AMPA ratio for AMPA receptor incorporation in distal apical and perisomatic dendrites of L2/3 PyNs. However, there was no rectification in distal apical or perisomatic synapses in L2/3 PyNs from 3-week-old rats (Fig. 8). Reversal potential and AMPA/NMDA ratios were similar between distal apical and perisomatic synapses. These results indicate that molecular compositions of AMPA and NMDA receptors are similar between distal apical and perisomatic dendrites in L2/3 PyNs of the primary visual cortex. However, since we investigated these properties at the third week of age, age profiles of these properties needs to be studied in the future.

Physiological implication

Long-term synaptic plasticity is one of candidate mechanisms of critical period associated with ocular dominance plasticity, which is a model for postnatal development of the sensory cortex. LTP and LTD in the primary visual cortex are layer dependent [45,46]. LTP and LTD in layer 4 neurons are lost shortly after eye opening while those in layer 2/3 continued beyond puberty in layer 2/3 in mice [47]. In our previous experiment, extracellular stimulation recruiting the less inhibitory influence could induce LTP and LTD in supragranular layer (layer 2/3) of 5-week-old rats at the end of critical period [48]. Modular architecture of cortical areas as a column is also characterized by hierarchical organization with higher cortical areas [6]. Top-down associative connections between cortical areas are important for brain functions such as priming and prediction [5]. These associative inputs are known to mainly terminate in layer 1 where distal apical dendrites of L2/3 and L5 PyNs receive synaptic terminals [49]. We have also reported that endocannabinoid signaling mediates muscarinic-induced LTD in perisomatic dendrites, but not in distal apical dendrites in L2/3 PyNs of the rat visual cortex [14]. These layer-specific properties and modulation of synaptic transmission in single pyramidal neurons adds more complexity to synaptic integration of concomitant associative and sensory information depending on neuromodulators associated with brain state [29]. Results of the present study should provide valuable information for layer-specific regulation of cortical information transfer.

ACKNOWLEDGEMENTS

This work was supported by a grant (2016R1A2B2016533) of the Basic Science Research Program through the National Research Foundation of Korea funded by the Ministry of Education, Science and Technology.

CONFLICTS OF INTEREST

The authors declare no conflicts of interest.

REFERENCES

1. Somogyi P, Tamás G, Lujan R, Buhl EH. Salient features of synaptic organisation in the cerebral cortex. *Brain Res Brain Res Rev.* 1998;26:113-135.
2. Williams SR, Stuart GJ. Role of dendritic synapse location in the control of action potential output. *Trends Neurosci.* 2003;26:147-154.
3. Sjöström PJ, Rancz EA, Roth A, Häusser M. Dendritic excitability and synaptic plasticity. *Physiol Rev.* 2008;88:769-840.
4. Spruston N. Pyramidal neurons: dendritic structure and synaptic integration. *Nat Rev Neurosci.* 2008;9:206-221.
5. Larkum M. A cellular mechanism for cortical associations: an organizing principle for the cerebral cortex. *Trends Neurosci.* 2013;36:141-151.
6. Shipp S. Structure and function of the cerebral cortex. *Curr Biol.* 2007;17:R443-R449.
7. Petreanu L, Mao T, Sternson SM, Svoboda K. The subcellular organization of neocortical excitatory connections. *Nature.* 2009;457:1142-1145.
8. Larkman AU. Dendritic morphology of pyramidal neurones of the visual cortex of the rat: III. Spine distributions. *J Comp Neurol.* 1991;306:332-343.

9. Larkum ME, Senn W, Lüscher HR. Top-down dendritic input increases the gain of layer 5 pyramidal neurons. *Cereb Cortex*. 2004;14:1059-1070.
10. Katz LC, Shatz CJ. Synaptic activity and the construction of cortical circuits. *Science*. 1996;274:1133-1138.
11. Bear MF, Rittenhouse CD. Molecular basis for induction of ocular dominance plasticity. *J Neurobiol*. 1999;41:83-91.
12. Cho KH, Jang HJ, Jo YH, Singer W, Rhie DJ. Cholinergic induction of input-specific late-phase LTP via localized Ca^{2+} release in the visual cortex. *J Neurosci*. 2012;32:4520-4530.
13. Salgado H, Garcia-Oscos F, Patel A, Martinolich L, Nichols JA, Dinh L, Roychowdhury S, Tseng KY, Atzori M. Layer-specific noradrenergic modulation of inhibition in cortical layer II/III. *Cereb Cortex*. 2011;21:212-221.
14. Joo K, Cho KH, Youn SH, Jang HJ, Rhie DJ. Layer-specific involvement of endocannabinoid signaling in muscarinic-induced long-term depression in layer 2/3 pyramidal neurons of rat visual cortex. *Brain Res*. 2019;1712:124-131.
15. Hasselmo ME. Neuromodulation: acetylcholine and memory consolidation. *Trends Cogn Sci*. 1999;3:351-359.
16. Wen JA, Barth AL. Input-specific critical periods for experience-dependent plasticity in layer 2/3 pyramidal neurons. *J Neurosci*. 2011;31:4456-4465.
17. Sarter M, Hasselmo ME, Bruno JP, Givens B. Unraveling the attentional functions of cortical cholinergic inputs: interactions between signal-driven and cognitive modulation of signal detection. *Brain Res Brain Res Rev*. 2005;48:98-111.
18. Gonchar Y, Burkhalter A. Three distinct families of GABAergic neurons in rat visual cortex. *Cereb Cortex*. 1997;7:347-358.
19. Brill J, Huguenard JR. Sequential changes in AMPA receptor targeting in the developing neocortical excitatory circuit. *J Neurosci*. 2008;28:13918-13928.
20. Quinlan EM, Olstein DH, Bear MF. Bidirectional, experience-dependent regulation of N-methyl-D-aspartate receptor subunit composition in the rat visual cortex during postnatal development. *Proc Natl Acad Sci U S A*. 1999;96:12876-12880.
21. Lee C, Joo K, Kim MJ, Rhie DJ, Jang HJ. GluN2B-containing N-methyl-D-aspartate receptors compensate for the inhibitory control of synaptic plasticity during the early critical period in the rat visual cortex. *J Neurosci Res*. 2015;93:1405-1412.
22. Rhie DJ, Kang HY, Ryu GR, Kim MJ, Yoon SH, Hahn SJ, Min DS, Jo YH, Kim MS. Electrophysiological and morphological classification of inhibitory interneurons in layer II/III of the rat visual cortex. *Korean J Physiol Pharmacol*. 2003;7:317-323.
23. Dobrunz LE, Stevens CF. Heterogeneity of release probability, facilitation, and depletion at central synapses. *Neuron*. 1997;18:995-1008.
24. Gil Z, Connors BW, Amitai Y. Differential regulation of neocortical synapses by neuromodulators and activity. *Neuron*. 1997;19:679-686.
25. Cruikshank SJ, Urabe H, Nurmikko AV, Connors BW. Pathway-specific feedforward circuits between thalamus and neocortex revealed by selective optical stimulation of axons. *Neuron*. 2010;65:230-245.
26. Rose HJ, Metherate R. Auditory thalamocortical transmission is reliable and temporally precise. *J Neurophysiol*. 2005;94:2019-2030.
27. Amitai Y. Thalamocortical synaptic connections: efficacy, modulation, inhibition and plasticity. *Rev Neurosci*. 2001;12:159-173.
28. Volpicelli LA, Levey AI. Muscarinic acetylcholine receptor subtypes in cerebral cortex and hippocampus. *Prog Brain Res*. 2004;145:59-66.
29. Lee SH, Dan Y. Neuromodulation of brain states. *Neuron*. 2012;76:209-222.
30. Hasselmo ME, McGaughy J. High acetylcholine levels set circuit dynamics for attention and encoding and low acetylcholine levels set dynamics for consolidation. *Prog Brain Res*. 2004;145:207-231.
31. Mesulam MM, Mufson EJ, Wainer BH, Levey AI. Central cholinergic pathways in the rat: an overview based on an alternative nomenclature (Ch1-Ch6). *Neuroscience*. 1983;10:1185-1201.
32. Lysakowski A, Wainer BH, Bruce G, Hersh LB. An atlas of the regional and laminar distribution of choline acetyltransferase immunoreactivity in rat cerebral cortex. *Neuroscience*. 1989;28:291-336.
33. van der Zee EA, Luiten PG. Muscarinic acetylcholine receptors in the hippocampus, neocortex and amygdala: a review of immunocytochemical localization in relation to learning and memory. *Prog Neurobiol*. 1999;58:409-471.
34. Alkondon M, Albuquerque EX. The nicotinic acetylcholine receptor subtypes and their function in the hippocampus and cerebral cortex. *Prog Brain Res*. 2004;145:109-120.
35. Hasselmo ME, Bower JM. Cholinergic suppression specific to intrinsic not afferent fiber synapses in rat piriform (olfactory) cortex. *J Neurophysiol*. 1992;67:1222-1229.
36. Hsieh CY, Cruikshank SJ, Metherate R. Differential modulation of auditory thalamocortical and intracortical synaptic transmission by cholinergic agonist. *Brain Res*. 2000;880:51-64.
37. Oldford E, Castro-Alamancos MA. Input-specific effects of acetylcholine on sensory and intracortical evoked responses in the "barrel cortex" *in vivo*. *Neuroscience*. 2003;117:769-778.
38. Jang HJ, Cho KH, Kim MJ, Yoon SH, Rhie DJ. Layer- and cell-type-specific tonic GABAergic inhibition of pyramidal neurons in the rat visual cortex. *Pflugers Arch*. 2013;465:1797-1810.
39. Liu G. Local structural balance and functional interaction of excitatory and inhibitory synapses in hippocampal dendrites. *Nat Neurosci*. 2004;7:373-379.
40. Haider B, Duque A, Hasenstaub AR, McCormick DA. Neocortical network activity *in vivo* is generated through a dynamic balance of excitation and inhibition. *J Neurosci*. 2006;26:4535-4545.
41. Lucas-Meunier E, Monier C, Amar M, Baux G, Frégnac Y, Fossier P. Involvement of nicotinic and muscarinic receptors in the endogenous cholinergic modulation of the balance between excitation and inhibition in the young rat visual cortex. *Cereb Cortex*. 2009;19:2411-2427.
42. Laezza F, Doherty JJ, Dingledine R. Long-term depression in hippocampal interneurons: joint requirement for pre- and postsynaptic events. *Science*. 1999;285:1411-1414.
43. Kumar SS, Bacci A, Kharazia V, Huguenard JR. A developmental switch of AMPA receptor subunits in neocortical pyramidal neurons. *J Neurosci*. 2002;22:3005-3015.
44. Busetto G, Higley MJ, Sabatini BL. Developmental presence and disappearance of postsynaptically silent synapses on dendritic spines of rat layer 2/3 pyramidal neurons. *J Physiol*. 2008;586:1519-1527.
45. Daw N, Rao Y, Wang XF, Fischer Q, Yang Y. LTP and LTD vary with layer in rodent visual cortex. *Vision Res*. 2004;44:3377-3380.
46. Wang XF, Daw NW. Long term potentiation varies with layer in rat visual cortex. *Brain Res*. 2003;989:26-34.
47. Jiang B, Treviño M, Kirkwood A. Sequential development of long-

term potentiation and depression in different layers of the mouse visual cortex. *J Neurosci.* 2007;27:9648-9652.
48. Jang HJ, Cho KH, Kim HS, Hahn SJ, Kim MS, Rhie DJ. Age-dependent decline in supragranular long-term synaptic plasticity by increased inhibition during the critical period in the rat primary visual cortex. *J Neurophysiol.* 2009;101:269-275.
49. Cauller L. Layer I of primary sensory neocortex: where top-down converges upon bottom-up. *Behav Brain Res.* 1995;71:163-170.